ONE-POT GREEN SYNTHESIS OF FLUORESCENT-QUANTUM CARBON DOTS FROM AVOCADO PEELS AND EVALUATION OF ITS ANTIMICROBIAL PROPERTIES

NANDIS FIALLOS[1], DIANA CORREA[1], SERGIO ACUÑA[2], MATIAS VENEGAS[1], FRANCISCO BUSTAMANTE[1], GIRLENNE CHRISTIANSEN[1], VANESA ROA[3], EDUARDO SCHOTT[3], JULIO ALARCÓN[1], AND EDGAR PASTENE [1]*

[1] *Laboratory of Synthesis and Natural Products, Department of Basic Sciences, Faculty of Sciences, University of Bío-Bío, Chillán, Chile.*
[2] *Facultad de Ciencias de la Salud y los Alimentos, University of Bío-Bío, Chillán, Chile.*
[3] *Departamento de Química Inorgánica, Facultad de Química y Farmacia, Centro de Energía UC, Centro de Investigación en Nanotecnología y Materiales Avanzados CIEN-UC, Pontificia Universidad Católica de Chile, Avenida Vicuña Mackenna, 4860 Santiago, Chile*.

ABSTRACT

In this work, avocado peel was chosen as a low-value waste that could be used as a carbon source to synthesize carbon dots (APCQDs). To obtain it, the hydrothermal method was used in the absence of co-doping agents. The synthesis was carried out for 6 hours at 250 ºC. After purification by dialysis and lyophilization, CQDs that exhibited intense blue fluorescence (emission at 378 nm) were obtained. Field emission scanning electron microscopy (FESEM), evidence the spherical morphology of carbon dots within nanometer range. HPLC analysis and separation showed excellent separation even in columns with low porosity, indicating a separation mechanism where polarity predominates as the property that governs the separation. It is highlighted that avocado peel CQDs have potent antimicrobial activity against the pathogens *Listeria monocytogenes* ATCC 7644, *Escherichia coli* ATCC 11775, *Staphylococcus aureus* ATCC 9144, and *Salmonella enterica* ATCC 13076. The antioxidant effect was also evidenced in the DPPH and ORAC-FL. The synthesis method for APCQDs could be easily scaled up for gram scale synthesis of carbon quantum dots.

Keywords: *Quantum carbon dots; Hydrothermal; Avocado peels*; HPLC.

1. INTRODUCTION

Science and technology have helped increase agricultural and industrial production. However, food waste on both the production and consumer sides has significantly increased. According to the Food Waste Index Report (https://bit.ly/UNEP-FWI-report), 931 million tons of food are wasted worldwide. These wastes correspond to complex, heterogeneous, biodegradable, and bioorganic substances that can be obtained from various sources such as perennial grasses, organic domestic waste, waste from agriculture, fishing, poultry, livestock, forestry, and related industries. Likewise, most of the residual biomass waste that is currently disposed of is either landfilled or burned in the open, which not only leads to wastage of resources but also causes some environmental problems that threaten human health [1]. Based on the concept of sustainability, the development of strategies to transform these wastes into useful materials is urgently needed. In view of the abovementioned, carbon quantum dots (CQDs) seem to be a good alternative to reduce the waste. In this regard, carbon dots (CQD) are a type of carbon nanoparticle that can be prepared from almost any animal and plant carbon source and that has gained great interest due to its ease of preparation and unlimited applications. Due to their extremely small size, high surface charge, tunable functional properties, and availability, CQDs have wide potential applications in biotechnology, biosensors, and foods, among others. Furthermore, they have shown that they can be synthesized in principle from any carbon-containing starting material, this ensures that most discard by-products from the food supply chain can be reused. These natural resources contain very diverse functional groups that contribute to the self-passivation of surface during the formation of CQDs nanoparticles. These materials can be produced hydrothermally, that is, by heating the starting material in water under atmospheric or elevated pressure. Other ways to obtain CDs are pyrolysis, and recently using microwaves (MW), pulsed electric fields (PEF) and ultrasound (US). However, the most convenient bottom-up method that allow a fine control of particle size is the reaction under hydrothermal conditions [2]. Likewise, the production cost is low, and the operation is easy and relatively safe and free of organic solvents [3–6]. Furthermore, shorter processing time and lower energy consumption can be obtained for CQDs manufacturing when using the other emerging methods (MW, PEF) as heat source. In this way, they can contribute beneficially to sustaining the development of nanotechnology and its applicability in various fields such as the conservation, security, and safety of various foods as an economic and sustainable technology. One of the most notable aspects of CQDs is their unlimited capacity to exhibit various chemical and pharmacological properties. Thus, these materials were initially used as chemiluminescent and fluorescent probes for imaging and biophotonics on cells, tissues, and organs. In addition, CQDs has low toxicity and specific subcellular distribution, properties that have quickly given them a place to be applied in biomedicine [7,8]. Interestingly, CQDs display pharmacological properties such as antitumor, antimicrobial, anti-inflammatory and even as a potential source of electrochemical energy [7–9]. These aspects can be reviewed in depth in recently published works [10,11]. Avocado fruit (*Persea Americana* Mill.) is one of the most important crops in South America and Chile. This fruit is known for its health benefits due to high levels of unsaturated fatty acids, minerals, fiber, proteins, carotenoids, vitamins, and polyphenols. Approximately, it is estimated that around six million tons of avocado are produced annually around the world, being the tropical fruit with the greatest growth in production in recent years. An average avocado is composed of pulp (between 65 and 73%), peel (between 11 and 15%) and seed (between 16 and 20%), [12,13]. However, the industry only uses the pulp to produce oil, puree, sauces, or snacks, generating large quantities of waste such as peel and seeds. These residues represent 25% of the total fruit, and within these the peel itself represents between 11% and 17% [14]. Avocado peel has been shown to be a rich source of bioactive polyphenolic compounds [13,15–17]. This byproduct is also a renewable, environmentally friendly, available, and harmless carbon source, which can be used to produce advanced biomaterials. Therefore, there is an opportunity to use avocado peel as a useful source to obtain CQDs. Furthermore, the presence of the various non-extractable polyphenolic compounds that are covalently linked to the lignocellulosic material of the avocado peel, can act as self-passivating agents of the surface of the CQDs during the synthesis. This advantage gives them a relatively high fluorescence quantum yield, excellent photostability, biocompatibility, low cytotoxicity, antioxidant, and antimicrobial activity, among others [18]. Synthesis and design of CQDs is very incipient and in our country, and only has been investigated at a fundamental level given its recognized lighting and catalytic properties. To date there are no direct applications in any productive sector. So, this work is the first in report this new approach to take advantage of low value raw materials and convert them into nanomaterials with great potential and diverse applications. The know-how can also be used to reconvert all types of carbon-based waste, which is widely supported in the literature [3–5,19]. In this work we seek to add value to an avocado by-product used as raw material for the synthesis of carbon quantum dots (CQDs). Through a simple hydrothermal transformation process, functional Carbon-Dots (CQD) are synthetized. Additionally, we evaluate peel-derived avocado CQDs as a new class of antimicrobials that can be used against pathogenic microorganisms.

2. EXPERIMENTAL

2.1 Vegetal material:

Avocado peels were obtained from mature fruits of *Persea americana* (var. Hass), purchased in local markets (march-November 2023) in the city of Chillán, Ñuble region, Chile. Peels were removed by hand al stored at -80ºC until used. Portions of avocado peels were freeze dried before the hydrothermal synthesis.

*Corresponding author email: epastene@ubiobio.cl

2.2 Green synthesis of Avocado Peel Quantum Carbon Dots (APCQD):

Freeze dried avocado peel (4 g) was milled in a blender during 1 min and transferred into a Teflon-lined stainless-steel autoclave. Double distilled water (40 mL) was introduced in the reactor with the avocado peel powder. The autoclave was tightly sealed, placed in an oven and heated at 250 °C for 6 h. After cool at room temperature, reactor was open, and the obtained product was filtered using filter paper. The solution obtained was then centrifuged at 9000 rpm for 30 min and finally filtered using PVDF membrane of 0.22 µm. This clear solution was freeze-dried for 48 h and the yield of the carbon dots was calculated from the initial amount of the starting material. The dark brown carbon quantum dots were stored in the fridge at 4 °C until characterization.

2.3 Instrumentation and characterization:

The UV-visible experiments were performed on a Shimadzu UV-2401PC UV–vis spectrophotometer. The infrared spectrum was measured using an ECO-ART Alpha Bruke Fourier transform infrared spectrometer. The X-ray diffraction (XRD) patterns were obtained with a Shimadzu 6000 diffractometer using Cu Kα radiation (λ = 0.15406 nm) as the X-ray source with a diffraction angle in the range 2θ (20–60°). Fluorescence excitation/emission spectra were recorded on Fluorimeter Perkin Elmer 6500. The morphological properties were studied by field emission scanning electron microscope (FESEM) using HITACHI SU3500 under an excitation energy of 5 and 1 kV.

2.4 HPLC:

HPLC analysis was performed using a YL9111S binary pump coupled to the YL9120s UV/Vis detector (Young Lin®, Korea). For the chromatography analysis, three columns were tested: 1) Kromasil KR100 column 100Å - 2.5 µm-C18, 4.6 mm x 50 mm; 2) Kromasil KR100 column 100Å - 3.5 µm-C18, 4.6 mm x 150 mm (Eka Chemicals AB, Bohus, Sweden), and 3) Cortecs column 90Å - 2.7 µm-C18, 4.6 mm x 150 mm (Waters, Milford, MA, USA). The solvent system was composed of solvent A (ultrapure water containing 0.5 % acetic, v/v) and solvent B (100% ACN). The gradient program was 0-5 min (2% B); 3-22 min (2-20% B); 22-24 min (20-30% B); 24-26 min (30-60% B); 26-32 min (60-2%B). Finally, the column was re-equilibrated or additional 5 min. The flow rate was 0.7 mL/min, and the injection volume was 20 µL. Detection was performed by using UV-VIS chromatograms acquired at 280 nm and 350 nm.

2.5 Antioxidant activity:

Free radical scavenging activity of avocado CQD was assessed by DPPH and ORAC-FL assays. The reduction of DPPH stable radical was kinetically monitored at 517 nm for 30 min [20]. The analyses were performed in the 96-well plate format using a 100 µmol/L DPPH solution (final concentration) in methanol. A 150 µL aliquot of DPPH reagent was added to the wells (except in the blank wells). Afterwards, 25 µL of samples, controls, or standard were added to each well. After mixing, readings were performed using an EPOCH microplate reader (BioTek Instruments). Data were analyzed with the Gen5 software package version 1.11. All determinations were performed in triplicates. The percentage of scavenging was calculated as:

$$\text{Scavenging DPPH rate} = \frac{1-(\text{A1}\ -\ \text{A2})}{\text{A0}}\ \text{x}\ 100\%$$

Where A0 is the absorbance of the control (DPPH without sample) and A1 is the absorbance in the presence of *APCQDs*, and A2 is the absorbance of sample without DPPH radical. The free radical scavenging ability of the samples was expressed as IC_{50} value, which is the inhibitory concentration at which 50% of DPPH radical was scavenged. The IC_{50} values were calculated from the area under the curve (AUC) of scavenging activities (%) vs the logarithm of concentrations of respective adducts. Trolox was used as control.

For the ORAC-FL trial, the previously published protocol [21] was applied, with slight modifications. 20 mL of the samples (Initial concentration 0.5 mg/mL) was diluted in 1 mL of 1X Phosphate saline buffer (PBS). The assay used 45 mL of diluted sample, 50 mL of 2,2'-azobis (2-amidino-propane) dihydrochloride AAPH (Cf = 18 mM in well), and 175 mL of fluorescein (Cf = 108 nM), so the final volume in this protocol is 270 mL. Before starting the readings, the radical was thermo-activated on the plate for 10 minutes (37°C) and then readings were taken every 3 minutes for 220 min. An excitation wavelength of 485 nm and an emission wavelength of 520 nm were applied in the assay, Trolox concentrations were 2.55-40.68 mM. The measurements were made in triplicate and only the average of the determinations is shown in the graphs for simplicity. The antioxidant capacity (ORAC) was calculated as follows:

$$ORAC\ =\ [(AUCs - AUCb)/(AUCtr\ -\ AUCb)].\,dilution\ factor\ [trolox]$$

Where AUCs is area under the curve of sample.

AUCb is area under the curve of blank.

AUCtr is area under the curve of Trolox solutions.

2.6 Antimicrobial Activity:

Susceptibility tests: For *Listeria monocytogenes* ATCC 7644, *Escherichia coli* ATCC 11775, *Staphylococcus aureus* ATCC 9144, and *Salmonella enterica* ATCC 13076, inoculum was spread using sterile swab on MRS agar plates, PALCAM and Müeller-Hinton, accordingly. Subsequently, Kirby-Bauer disk diffusion test was performed for *APCQD* sample. The circular disks (8 mm diameter) were first immersed in the solution of APCQDs (5 mg/mL, 500 mg per disk) for 30 minutes and then placed on the plates. Plates were incubated for 24 h at 37°C under aerobiosis conditions. Control antibiotic susceptibility disks of amoxicillin 30 µg, gentamicin 10 µg, and chloramphenicol 30 µg were used. All tests were performed in triplicate and the observed antibacterial activity was expressed as the average of the inhibition diameters (mm) produced by the tested samples [22]

2.7 Statistical analysis

Data were analyzed using the GraphPad Prism 4 statistical software. Values represent the means of at least three independent experiments, each conducted in quadruplicate. Data were analyzed by analysis of variance with post hoc comparison using Tukey's test.

3. RESULTS AND DISCUSSION

3.1. Characterization of APCQDs:

The UV–vis spectrum of carbon quantum dots presented in Fig. 1A, reveals a typical absorption spectrum of the synthesized CQDs. The main characteristics are the absorption peaks around 280 nm, which could correspond to the π–π* transition derived from the C=C bond [23]. With lower intensity, a broad peak is observed around 320-360 nm, probably generated by the n–π* transition of the C═O bond. In Figure 1B, fluorescence spectrum is depicted, showing an intense emission band around 378 nm [24]. The lighting properties of carbon dots have been by far the most researched. Apart from the obvious applications in imaging, these properties are linked to certain biological properties, such as antimicrobial activities. It is known that, in CQDs, more than the nature of the side chains that decorate the surface, the hybridization of the carbon skeleton and the chemical groups connected to them is important. When completely carbonized, the surface functional groups and side chains disappear, with the size effect predominating in this condition. Thus, in CQDs with a solid core, the fluorescence emission is controlled by adjusting the functional groups of the inner core and the surface. Basically, the fluorescence can be tuned by adjusting the ratio of sp2/sp3 carbons within the CQDs [24–26].

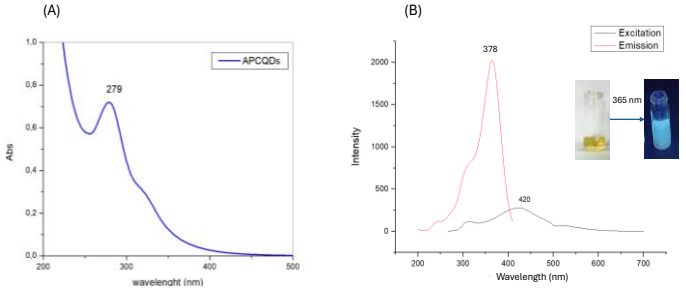

Figure 1. (A) UV-vis spectrum of Avocado Peel Quantum Carbon Dots (APQCDs), (B) excitation, and emission spectra of Avocado Peel Quantum Carbon Dots (APQCDs). Inset Figure 1B photography of the blue/green-emitting APCQDs under sunlight (left) and UV irradiation (right).

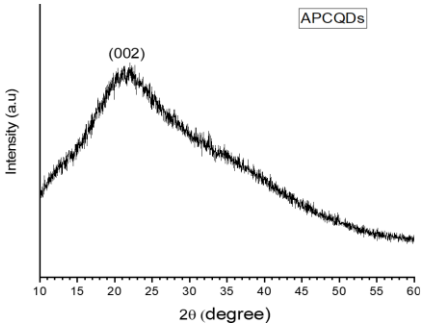

Figure 2. X-ray diffraction (XDR), pattern of Avocado Peel Quantum Carbon Dots (APQCDs).

The XRD measurements help to identify semi-crystalline structure in CDAs with (002) planes of graphene in between amorphous regions The diffraction pattern of the synthesized carbon APCQDs presented in Fig. 2 shows the peaks at 2θ = 24.5° that correspond to the (002) plane of carbonaceous materials. The (002) plane is attributed to the arrangement of disordered carbon atoms within the hexagonal graphite structure of carbon quantum dots, leading to the formation of a turbostratic structure through interlayer packing. The presence of this broad peak and relatively high value of interlayer distance of 0.34 nm also indicate oxygen- containing functionalities [23,27,28].

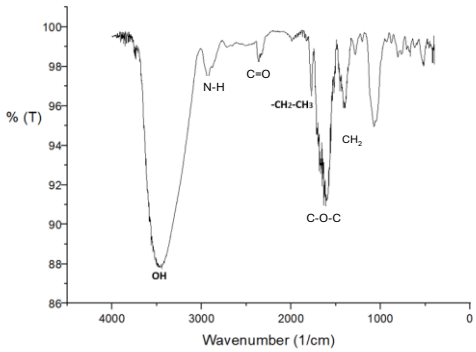

Figure 3. FTIR spectrum of Avocado Peel Quantum Carbon Dots (APQCDs).

Figure 3 shows the FTIR spectra of APCQDs, which showed a typical band at 3457 cm^{-1}, which can be unambiguously assigned to stretching vibrations of O-H. This signal indicates the existence of water absorbed on the surface of the APQCD. Another distinctive bands could be observed at 1637 cm^{-1}, 1371 cm^{-1} and 1023 cm^{-1}, corresponding to the vibrations of C=C, C-O, and C-O-C bonds, respectively. These band are attributed to asymmetric and symmetric stretching vibrations of COO− group, respectively. A sharp peak at 2932 cm^{-1} suggested the formation of N-H vibrational. These bands reveal the surface functional groups present at the APQCDs. Therefore, the FTIR results indicated that the surfaces of carbon dots were full hydrophilic and presented mainly hydroxyl and carbonyl groups. The hydrophilic surface explains the highly dispersibility in water of APCQDs.

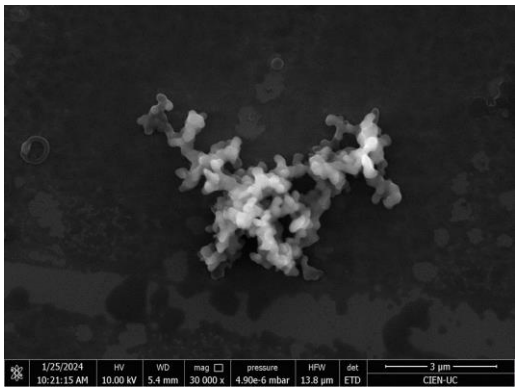

Figure 4. FESEM image of APCQDs at 3 mm scale.

According to the FESEM image depicted in Fig. 4, the APCQDs were observed to have discrete spherical particles that exhibited fine features. The homogeneity observed in the samples indicates that the synthesis method was optimal and that the particles were resistant to aggregation, indicating stability [29]. Round shaped carbon nanodots on the surface have an average diameter below 10 nm.

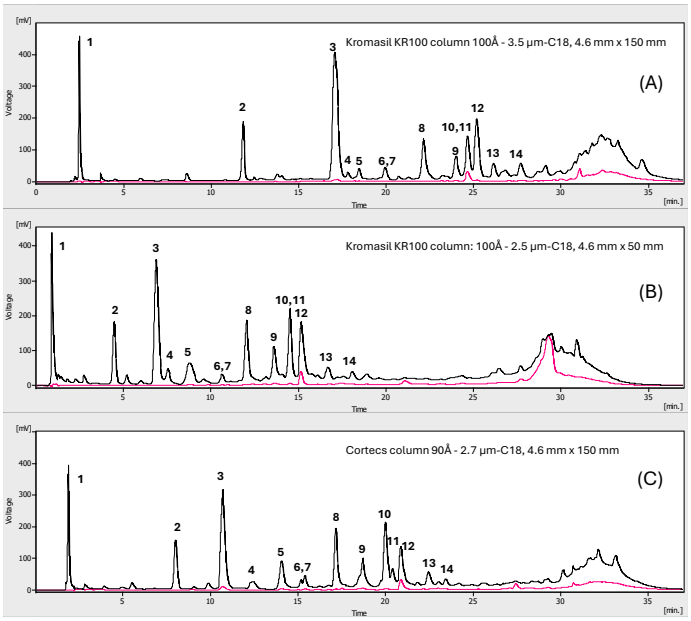

Figure 4. HPLC trace of APCQDs obtained after hydrothermal processing. (A) Fully porous 100 Å particle 0f 3.5 µm diameter (B); Fully porous 100 Å, particle of 2.5 µm diameter and, (C); Core-shell with superficial porosity 90 Å, particle of 2.7 µm diameter.

3.2 High Performance Liquid Chromatography (HPLC):

A separation of the APCQDs fractionated by reversed phase HPLC is illustrated in Figure 4. Fourteen major peaks can be observed, which show absorption in the UV region (280 and 350 nm). Although column or thin layer chromatography was not initially considered the technique of choice to separate this type of nanoparticles, recent studies have positioned it as a technique with high potential. Normally, separation methods based on size exclusion (SEC) are the logical choice and, in most articles, published in the last 5 years, dialysis and ultrafiltration are part of the mandatory protocols in CDs purification. However, there are some criticisms of these methodologies, among which we can mention their scaling problems and uncertainty regarding the actual separation of CDs from other molecular fluorophores that can pass through dialysis membranes. Thus, it is currently suggested to use supportive techniques to guarantee CDs purification, such as the use of NMR and XPS. Electrophoresis and conventional column chromatography allows separation based on mixed mechanisms including charge/size, polarity, and size exclusion (SEC) [30]. For this reason, a parameter that must be considered when choosing the column over particle size is porosity. In our study, we used two columns with a particle size of 2.5 and 3,5 µm (Figure 4 AB) and pore size of 100 Å (10 nm). Since after the hydrothermal process there is an elimination of particles larger than 220 nm (PVDF membrane filtration), the CQDs that remain in suspension have a size range between 4-10 nm, which allows SEC phenomena operate inside the spherical particles of HPLC column. If the above occurs, one can assume that the first peak cluster (1), which are poorly retained in the HPLC column, correspond to carbon particles larger than 10 nm. One of the first pioneering works on the use of HPLC to separate CDs was that of Lu et al, [31]. They used a C18 column packed with particles containing 8 nm pores. Among the main findings of this study, it can be mentioned that there is indeed a mixed mechanism of separation by SEC and polarity like any other organic compound, but very dependent on flow and temperature. Thus, temperatures greater than 25ºC impair the separation, as do flows that exceed 1.4 mL/min. In our study, for the three columns, a maximum flow of 0.7 mL/min and 25ºC were used, which were maintained with the column oven. As mentioned earlier in the text, the importance of pores in silica particles seems to be central for the separation of CQDs. To confirm this statement, the

same HPLC methodology was used to separate the APCQDs in an HPLC column filled with core shell particles [32], that is, the particles only have surface porosity, and the stationary phase is distributed in a thin layer [33]. Thus, the separation of CQDs will be mainly driven by interactions of their functional groups with the C-18 phase. In the column with fully porous particles, the separation is affected by slow mass transfer from mobile phase through to the stationary phase and back again. In core shell particles this effect is dramatically reduced since diffusion of the target compounds only occurs in the outer layer and the movement between particles is very limited. Compared to the fully porous particles of conventional columns, the core shell particles used in our study have around 81.5% solid core and 18.5% porous surface layer. If indeed the presence of pores is important to promote SEC, a higher separation would not be expected in core shell columns. On the contrary, in our study, solid core columns seem to achieve better separation compared to fully porous ones (Figure 4C). This suggests that, at least in reversed-phase HPLC, APCQDs are separated primarily by interaction with octadecylsilyl (C-18) groups rather than SEC. Despite the lower porosity of the core shell particles, the SEC phenomenon cannot be completely ruled out. Indeed, the negative effect on separation associated with low porosity can be compensated by the greater efficiency displayed by these columns [34]. Overall, it is important to highlight that one of the advantages of using HPLC is the possibility of scale-up the separation Unfortunately, the small load capacity of core shell columns limits this technology to a purely analytical field. However, its potential for CQD characterization deserves to be explored further. Therefore, preparative HPLC could be an attractive choice not only with the aim to study bioactivities but also to characterize CDs individually, since it has been reported that when using this purification method, the quantum yields are higher than when dialysis is used, probably due to the presence of impurities that quench fluorescence [35,36].

3.3 Antimicrobial Activity:

The efficacy of APQCDs was evaluated by various tests on Gram positive and negative strains. Bacterial susceptibility was analyzed on agar plates using a final concentration of 500 µg APCQDs per disk. According to the results presented in Table 1, the sample of avocado CQDs synthesized in the present study showed potent antibacterial activity at the concentration of 500 µg/mL. This effect was evident against all the bacterial strains considered in the test. In general, looking at the Figure 4, it can be confirmed that the effect is comparable to that of the antibiotics used as a control.

Table 1. Results of antimicrobial susceptibility tests for APCQDs against different pathogenic bacteria.

Samples/Controls	***Salmonella spp***	***Escherichia coli spp***	***Staphylococcus aureus***	***Listeria monocytogenes***
	Zone of inhibition (Mean ± SD, mm)			
APCQs (500 mg/mL)	25 ± 0.6	40 ± 0.5	24	35
Positive control GE (10 µg/mL)	25 ± 0.5	35 ± 0.2	22	38
Positive control CC (30 µg/mL)	25 ± 0.8	27 ± 0.2	25	30

GE: Gentamicyn disks. CC: Cloramphenicol disks

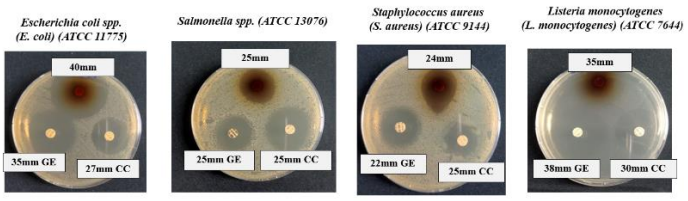

Figure 4. Growth inhibition of pathogenic bacterial strains caused by APCQDs.

The central structure and surface functional groups of CQDs determine their functional and biological properties. In particular, the bactericidal or bacteriostatic action of CQDs originates mainly through three routes [37,38]: (1) physical and mechanical damage to the bacterial cell wall and membrane with consequent leakage of cytoplasmic material; (2) direct or light-promoted generation of highly reactive oxygen species (ROS); (3) inhibition of cell proliferation through damage to genetic material (DNA/RNA) and proteins. Furthermore, the antibacterial efficacy of CQDs will depend on the structure, precursors, synthetic methods, functionalization, size, doping, shape, zeta potential and surface charge effects. Regarding the disruption of the cell wall and membrane, it is known that the penetration of CQDs through the bacterial cell wall and membrane is related to the interaction with the phospholipid bilayer. This interaction causes the membrane to become rougher and shrink, causing the rupture and discharge of its cellular components to the outside (lysis). ROS production by CQDs is related to their photosensitizing properties. Thus, the high electron transfer with large amounts of free electrons and holes facilitates the generation of highly toxic radicals for the bacteria. Furthermore, ultraviolet, or visible light catalyzes these processes and leads to bacterial oxidative stress, inhibiting their respiration and replication. It is accepted that the cell death promoting mechanism is apoptotic type characterized by the formation and accumulation of hydrogen peroxide (H_2O_2), hydroxyl anions (OH-), superoxide anion ($O_2^{\cdot-}$) and triplet oxygen ($^3O_2$) [39,40]. Recent studies suggest that CQDs that have carboxylic groups on their surface have intrinsic peroxidase activity (peroxidase-like behavior) [41]. Furthermore, this activity can be amplified using Fe in N-doped CDs, which can be used in the development of various types of sensors [42,43]. The direct interaction with the genetic material and the accumulation of CQDs in the nucleus of eukaryotic cells has been reported in several works [44,45]. In the case of bacterium, this interaction is faster and allows the inhibition of cellular respiration, division, replication, and production of adenosine triphosphate (ATP), which results in necrosis/apoptosis and eventual bacterial death. According to recent literature, this mechanism is most relevant for N-doped CQDs. In this type of CQDs, the interaction with DNA is mainly due to electrostatic adsorption. Other forces that also contribute to this biomolecular interaction are the nucleobase effect, hydrophobic interaction, and van der Waals forces [46,47].

3.4 Antioxidant Activity:

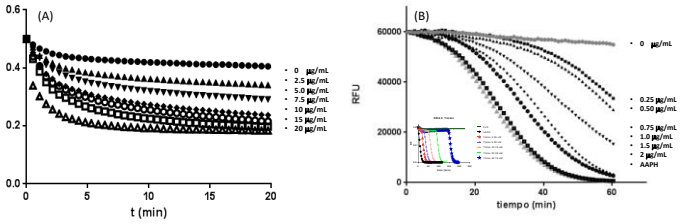

Figure 5. (A) DPPH assay for APCQDs, (B) ORAC-FL assay for APCQDs. Inset in (B) corresponds to ORAC-FL calibration with 2.6-40.8 mM Trolox.

The antioxidant activity of CD has been reported in several preliminary works. It is interesting that the same nanomaterial has an oxidant-antioxidant effect [48]. However, it should be emphasized that this dual property of CQDs cannot be extrapolated to all CQDs and depends on the raw material of origin and the functional groups that are available on its surface. The incident light (typically blue between 390–470 nm) and the chemical environment also determine the appearance of one effect or another [49]. Furthermore, within the cluster of different CQDs present in our sample of APCQDs it is very likely that some are ROS generators and others behave as antioxidants [50,51]. For this reason, to answer this question it is mandatory to separate them using an appropriate method and evaluate them individually. In the DPPH assay the IC_{50} value was 6.2 ug/mL, while the ORAC value in trolox equivalents was 8.2 mmol/g. The traditional ORAC assay can be used in the case of CQDs that emit above 520 nm, however, it should be considered that CQDs with emissions close to the fluorescein emission could be complex to interpret. In this case, a different assay should be used, or the probe replaced with pyrogallol red [52].

CONCLUSIONS

In this work, carbon quantum dots (CQDs) were prepared from avocado peel using the classic hydrothermal method. The CQDs obtained were dialyzed and once suspended in water they showed intense blue fluorescence. Its antimicrobial properties on pathogenic bacteria allow us to propose that this type of nanomaterial can be used to control microorganisms in food or as a basis for the

design of nanoparticles for medical purposes. The ability to neutralize the DPPH radical and protect fluorescein from oxidation induced by AAPH suggests that these nanoparticles can also help slow down deterioration processes or damage associated with free radicals. Finally, HPLC analysis using columns with completely porous particles and core-shell particles with superficial porosity, allowed the separation of the CQDs based on their polarity. This result indicates that chromatographic separation can be of great potential for the study of individual CQDs, to elucidate their biological properties in the absence of quenchers**.**

ACKNOWLEDGMENTS

This work was supported by Grants: Cs2030 I+D 23-24, regular project (#1211119) from FONDECYT, and FONDEQUIP EQM200098 from ANID, the Chilean National Research and Development Agency. ANID/FONDAP/1523A0006. ACT210057. FONDECYT 1231719.

REFERENCES

1. Meng, W.; Bai, X.; Wang, B.; Liu, Z.; Lu, S.; Yang, B. Biomass-Derived Carbon Dots and Their Applications. ENERGY & ENVIRONMENTAL MATERIALS 2019, 2, 172–192, doi:10.1002/eem2.12038.
2. Banger, A.; Gautam, S.; Jadoun, S.; Jangid, N.K.; Srivastava, A.; Pulidindi, I.N.; Dwivedi, J.; Srivastava, M. Synthetic Methods and Applications of Carbon Nanodots. Catalysts 2023, 13, 858, doi:10.3390/catal13050858.
3. Prasannan, A.; Imae, T. One-Pot Synthesis of Fluorescent Carbon Dots from Orange Waste Peels. Ind Eng Chem Res 2013, 52, 15673–15678, doi:10.1021/ie402421s.
4. de Oliveira, B.P.; da Silva Abreu, F.O.M. Carbon Quantum Dots Synthesis from Waste and By-Products: Perspectives and Challenges. Mater Lett 2021, 282, 128764, doi:10.1016/j.matlet.2020.128764.
5. Khairol Anuar, N.K.; Tan, H.L.; Lim, Y.P.; So'aib, M.S.; Abu Bakar, N.F. A Review on Multifunctional Carbon-Dots Synthesized From Biomass Waste: Design/ Fabrication, Characterization and Applications. Front Energy Res 2021, 9, doi:10.3389/fenrg.2021.626549.
6. Cailotto, S.; Massari, D.; Gigli, M.; Campalani, C.; Bonini, M.; You, S.; Vomiero, A.; Selva, M.; Perosa, A.; Crestini, C. N-Doped Carbon Dot Hydrogels from Brewing Waste for Photocatalytic Wastewater Treatment. ACS Omega 2022, 7, 4052–4061, doi:10.1021/acsomega.1c05403.
7. Sharma, A.; Das, J. Small Molecules Derived Carbon Dots: Synthesis and Applications in Sensing, Catalysis, Imaging, and Biomedicine. J Nanobiotechnology 2019, 17, 92, doi:10.1186/s12951-019-0525-8.
8. Gedda, G.; Bhupathi, A.; Balaji Gupta Tiruveedhi, V.L.N. Naturally Derived Carbon Dots as Bioimaging Agents. In Biomechanics and Functional Tissue Engineering; IntechOpen, 2021.
9. Han, L.; Guo, Y.; Zhang, H.; Wang, Z.; Zhang, F.; Wang, Y.; Li, X.; Wang, Y.; Ye, J. Preparation of Carbon Quantum Dot Fluorescent Probe from Waste Fruit Peel and Its Use for the Detection of Dopamine. RSC Adv 2024, 14, 1813–1821, doi:10.1039/D3RA06799H.
10. Khairol Anuar, N.K.; Tan, H.L.; Lim, Y.P.; So'aib, M.S.; Abu Bakar, N.F. A Review on Multifunctional Carbon-Dots Synthesized From Biomass Waste: Design/ Fabrication, Characterization and Applications. Front Energy Res 2021, 9, doi:10.3389/fenrg.2021.626549.
11. Liu, J.; Li, R.; Yang, B. Carbon Dots: A New Type of Carbon-Based Nanomaterial with Wide Applications. ACS Cent Sci 2020, 6, 2179–2195, doi:10.1021/acscentsci.0c01306.
12. Figueroa, J.G.; Borrás-Linares, I.; Del Pino-García, R.; Curiel, J.A.; Lozano-Sánchez, J.; Segura-Carretero, A. Functional Ingredient from Avocado Peel: Microwave-Assisted Extraction, Characterization and Potential Applications for the Food Industry. Food Chem 2021, 352, 129300, doi:10.1016/j.foodchem.2021.129300.
13. Saavedra, J.; Córdova, A.; Navarro, R.; Díaz-Calderón, P.; Fuentealba, C.; Astudillo-Castro, C.; Toledo, L.; Enrione, J.; Galvez, L. Industrial Avocado Waste: Functional Compounds Preservation by Convective Drying Process. J Food Eng 2017, 198, 81–90, doi:10.1016/j.jfoodeng.2016.11.018.
14. Araújo, R.G.; Rodriguez-Jasso, R.M.; Ruiz, H.A.; Pintado, M.M.E.; Aguilar, C.N. Avocado By-Products: Nutritional and Functional Properties. Trends Food Sci Technol 2018, 80, 51–60, doi:10.1016/j.tifs.2018.07.027.
15. Calderón-Oliver, M.; Escalona-Buendía, H.B.; Medina-Campos, O.N.; Pedraza-Chaverri, J.; Pedroza-Islas, R.; Ponce-Alquicira, E. Optimization of the Antioxidant and Antimicrobial Response of the Combined Effect of Nisin and Avocado Byproducts. LWT - Food Science and Technology 2016, 65, 46–52, doi:10.1016/j.lwt.2015.07.048.
16. Segovia, F.J.; Corral-Pérez, J.J.; Almajano, M.P. Avocado Seed: Modeling Extraction of Bioactive Compounds. Ind Crops Prod 2016, 85, 213–220, doi:10.1016/j.indcrop.2016.03.005.
17. Chávez, F.; Aranda, M.; García, A.; Pastene, E. Antioxidant Polyphenols Extracted from Avocado Epicarp (Persea Americana Var. Hass) Inhibit Helicobacter Pylori Urease. Bol Latinoam Caribe Plantas Med Aromat 2011, 10.
18. Cui, L.; Ren, X.; Sun, M.; Liu, H.; Xia, L. Carbon Dots: Synthesis, Properties and Applications. Nanomaterials 2021, 11, 3419, doi:10.3390/nano11123419.
19. Kuang, T.; Jin, M.; Lu, X.; Liu, T.; Vahabi, H.; Gu, Z.; Gong, X. Functional Carbon Dots Derived from Biomass and Plastic Wastes. Green Chemistry 2023, 25, 6581–6602, doi:10.1039/D3GC01763J.
20. Mishra, K.; Ojha, H.; Chaudhury, N.K. Estimation of Antiradical Properties of Antioxidants Using DPPH Assay: A Critical Review and Results. Food Chem 2012, 130, 1036–1043, doi:10.1016/j.foodchem.2011.07.127.
21. Kassim, N.K.; Rahmani, M.; Ismail, A.; Sukari, M.A.; Ee, G.C.L.; Nasir, N.M.; Awang, K. Antioxidant Activity-Guided Separation of Coumarins and Lignan from Melicope Glabra (Rutaceae). Food Chem 2013, 139, 87–92, doi:10.1016/j.foodchem.2013.01.108.
22. Adhikari, B.; Shah, P.K.; Karki, R. Antibiogram and Phytochemical Analysis of Cinnamon, Clove, and Sichuan Pepper Extracts. Nepal Journal of Biotechnology 2021, 9, 1–7, doi:10.3126/njb.v9i1.38644.
23. Kumar, M.S.; Yasoda, K.Y.; Kumaresan, D.; Kothurkar, N.K.; Batabyal, S.K. TiO 2 -Carbon Quantum Dots (CQD) Nanohybrid: Enhanced Photocatalytic Activity. Mater Res Express 2018, 5, 075502, doi:10.1088/2053-1591/aacbb9.
24. Wang, B.; Lu, S. The Light of Carbon Dots: From Mechanism to Applications. Matter 2022, 5, 110–149, doi:10.1016/j.matt.2021.10.016.
25. Rooj, B.; Mandal, U. A Review on Characterization of Carbon Quantum Dots. Vietnam Journal of Chemistry 2023, 61, 693–718, doi:10.1002/vjch.202300022.
26. Ren, J.; Stagi, L.; Innocenzi, P. Fluorescent Carbon Dots in Solid-State: From Nanostructures to Functional Devices. Progress in Solid State Chemistry 2021, 62, 100295, doi:10.1016/j.progsolidstchem.2020.100295.
27. Shaikh, A.F.; Tamboli, M.S.; Patil, R.H.; Bhan, A.; Ambekar, J.D.; Kale, B.B. Bioinspired Carbon Quantum Dots: An Antibiofilm Agents. J Nanosci Nanotechnol 2019, 19, 2339–2345, doi:10.1166/jnn.2019.16537.
28. Döring, A.; Ushakova, E.; Rogach, A.L. Chiral Carbon Dots: Synthesis, Optical Properties, and Emerging Applications. Light Sci Appl 2022, 11, 75, doi:10.1038/s41377-022-00764-1.
29. Kumari, M.; Chaudhary, G.R.; Chaudhary, S.; Huang, M.; Guo, Z. Transformation of Waste Rice Straw to Carbon Quantum Dots and Their Potential Chemical Sensing Application: Green and Sustainable Approach to Overcome Stubble Burning Issues. Biomass Convers Biorefin 2022, doi:10.1007/s13399-022-02761-1.
30. Ding, H.; Yu, S.-B.; Wei, J.-S.; Xiong, H.-M. Full-Color Light-Emitting Carbon Dots with a Surface-State-Controlled Luminescence Mechanism. ACS Nano 2016, 10, 484–491, doi:10.1021/acsnano.5b05406.
31. Lu, Y.; Wang, J.; Yuan, H.; Xiao, D. Separation of Carbon Quantum Dots on a C18 Column by Binary Gradient Elution via HPLC. Anal. Methods 2014, 6, 8124–8128, doi:10.1039/C4AY01052C.
32. Hayes, R.; Ahmed, A.; Edge, T.; Zhang, H. Core–Shell Particles: Preparation, Fundamentals and Applications in High Performance Liquid Chromatography. J Chromatogr A 2014, 1357, 36–52, doi:10.1016/j.chroma.2014.05.010.
33. Oláh, E.; Fekete, S.; Fekete, J.; Ganzler, K. Comparative Study of New Shell-Type, Sub-2μm Fully Porous and Monolith Stationary Phases, Focusing on Mass-Transfer Resistance. J Chromatogr A 2010, 1217, 3642–3653, doi:10.1016/j.chroma.2010.03.052.
34. Pirok, B.W.J.; Breuer, P.; Hoppe, S.J.M.; Chitty, M.; Welch, E.; Farkas, T.; van der Wal, S.; Peters, R.; Schoenmakers, P.J. Size-Exclusion Chromatography Using Core-Shell Particles. J Chromatogr A 2017, 1486, 96–102, doi:10.1016/j.chroma.2016.12.015.
35. Chen, C.-Y.; Tsai, Y.-H.; Chang, C.-W. Evaluation of the Dialysis Time Required for Carbon Dots by HPLC and the Properties of Carbon Dots after HPLC Fractionation. New Journal of Chemistry 2019, 43, 6153–6159, doi:10.1039/C9NJ00434C.

36. Gong, X.; Hu, Q.; Paau, M.C.; Zhang, Y.; Shuang, S.; Dong, C.; Choi, M.M.F. Red-Green-Blue Fluorescent Hollow Carbon Nanoparticles Isolated from Chromatographic Fractions for Cellular Imaging. Nanoscale 2014, 6, 8162, doi:10.1039/c4nr01453g.
37. Lin, F.; Wang, Z.; Wu, F.-G. Carbon Dots for Killing Microorganisms: An Update since 2019. Pharmaceuticals 2022, 15, 1236, doi:10.3390/ph15101236.
38. Ghirardello, M.; Ramos-Soriano, J.; Galan, M.C. Carbon Dots as an Emergent Class of Antimicrobial Agents. Nanomaterials 2021, 11, 1877, doi:10.3390/nano11081877.
39. Norouzi, N.; Nusantara, A.C.; Ong, Y.; Hamoh, T.; Nie, L.; Morita, A.; Zhang, Y.; Mzyk, A.; Schirhagl, R. Relaxometry for Detecting Free Radical Generation during Bacteria's Response to Antibiotics. Carbon N Y 2022, 199, 444–452, doi:10.1016/j.carbon.2022.08.025.
40. Dong, X.; Liang, W.; Meziani, M.J.; Sun, Y.-P.; Yang, L. Carbon Dots as Potent Antimicrobial Agents. Theranostics 2020, 10, 671–686, doi:10.7150/thno.39863.
41. Das, S.; Ngashangva, L.; Mog, H.; Gogoi, S.; Goswami, P. An Insight into the Mechanism of Peroxidase-like Activity of Carbon Dots. Opt Mater (Amst) 2021, 115, 111017, doi:10.1016/j.optmat.2021.111017.
42. Bandi, R.; Alle, M.; Dadigala, R.; Park, C.-W.; Han, S.-Y.; Kwon, G.-J.; Kim, J.-C.; Lee, S.-H. Integrating the High Peroxidase Activity of Carbon Dots with Easy Recyclability: Immobilization on Dialdehyde Cellulose Nanofibrils and Cholesterol Detection. Appl Mater Today 2022, 26, 101286, doi:10.1016/j.apmt.2021.101286.
43. Yuan, C.; Qin, X.; Xu, Y.; Li, X.; Chen, Y.; Shi, R.; Wang, Y. Carbon Quantum Dots Originated from Chicken Blood as Peroxidase Mimics for Colorimetric Detection of Biothiols. J Photochem Photobiol A Chem 2020, 396, 112529, doi:10.1016/j.jphotochem.2020.112529.
44. Jacinth Gracia, K.D.; Thavamani, S.S.; Amaladhas, T.P.; Devanesan, S.; Ahmed, M.; Kannan, M.M. Valorisation of Bio-Derived Fluorescent Carbon Dots for Metal Sensing, DNA Binding and Bioimaging. Chemosphere 2022, 298, 134128, doi:10.1016/j.chemosphere.2022.134128.
45. Travlou, N.A.; Giannakoudakis, D.A.; Algarra, M.; Labella, A.M.; Rodríguez-Castellón, E.; Bandosz, T.J. S- and N-Doped Carbon Quantum Dots: Surface Chemistry Dependent Antibacterial Activity. Carbon N Y 2018, 135, 104–111, doi:10.1016/j.carbon.2018.04.018.
46. Daphne Jacinth Gracia, K.; Muthukumar Sivaraman, R.; Sheeba Thavamani, S.; Peter Amaladhas, T.; Devanesan, S.; AlSalhi, M.S.; Balakrishnan, M. Nitrogen Doped Fluorescent Carbon Dots from Delonix Regia for Fe(III) and Cysteine Sensing, DNA Binding and Bioimaging. Arabian Journal of Chemistry 2023, 16, 105109, doi:10.1016/j.arabjc.2023.105109.
47. Li, F.; Cai, Q.; Hao, X.; Zhao, C.; Huang, Z.; Zheng, Y.; Lin, X.; Weng, S. Insight into the DNA Adsorption on Nitrogen-Doped Positive Carbon Dots. RSC Adv 2019, 9, 12462–12469, doi:10.1039/C9RA00881K.
48. Christensen, I.L.; Sun, Y.-P.; Juzenas, P. Carbon Dots as Antioxidants and Prooxidants. J Biomed Nanotechnol 2011, 7, 667–676, doi:10.1166/jbn.2011.1334.
49. Innocenzi, P.; Stagi, L. Carbon Dots as Oxidant-Antioxidant Nanomaterials, Understanding the Structure-Properties Relationship. A Critical Review. Nano Today 2023, 50, 101837, doi:10.1016/j.nantod.2023.101837.
50. Li, J.; Zhou, Y.; Xiao, Y.; Cai, S.; Huang, C.; Guo, S.; Sun, Y.; Song, R.-B.; Li, Z. Carbon Dots as Light-Responsive Oxidase-like Nanozyme for Colorimetric Detection of Total Antioxidant Capacity in Fruits. Food Chem 2023, 405, 134749, doi:10.1016/j.foodchem.2022.134749.
51. Gao, F.; Liu, J.; Gong, P.; Yang, Y.; Jiang, Y. Carbon Dots as Potential Antioxidants for the Scavenging of Multi-Reactive Oxygen and Nitrogen Species. Chemical Engineering Journal 2023, 462, 142338, doi:10.1016/j.cej.2023.142338.
52. Ortiz, R.; Antilén, M.; Speisky, H.; Aliaga, M.E.; López-Alarcón, C.; Baugh, S. Application of a Microplate-Based ORAC-Pyrogallol Red Assay for the Estimation of Antioxidant Capacity: First Action 2012.03. J AOAC Int 2012, 95, 1558–1561, doi:10.5740/jaoacint.CS2012_03.